

An Impact Study of FORMOSAT-3/COSMIC GPS Radio Occultation and Dropsonde Data on WRF Simulations

Fang-Ching Chien

*Department of Earth Sciences
National Taiwan Normal University
Taipei, TAIWAN*

Ying-Hwa Kuo

*Mesoscale & Microscale Meteorology (MMM) Division
National Center for Atmospheric Research
Boulder, CO 80307-3000*

Abstract

This paper presents the result of a cooperative study under the Integrated Research Project of FORMOSAT-3/COSMIC and SoWMEX (Southwest Monsoon Experiment) in Taiwan. We focus on the comparison and impact studies of FORMOSAT-3 GPS radio occultation and dropsonde data on regional weather prediction. The WRF model and its 3DVAR component, WRF Var, are used for evaluation on the forecast of heavy rainfall events in Taiwan during an 11-day period of the 2007 Mei-yu season. The result shows that the GPS data tend to improve the simulations for longer integration, e.g., after 36 h. The best performance is on correcting the under-prediction of geopotential height. The dropsonde data help to improve the simulation only at earlier forecast time and at higher levels (e.g., 500 and 300 hPa). With both the GPS and the dropsonde data assimilated together, the simulation shows even more improvement. At 12-24 h, there is no impact of GPS and dropsonde data on rainfall forecasts. However, when the integration time getting longer, the GPS and dropsonde data starts to help the rainfall simulation, especially for small rain thresholds.

1. Introduction

This paper presents the result of a cooperative study under the Integrated Research Project of FORMOSAT-3/ COSMIC and SoWMEX (Southwest Monsoon Experiment) in Taiwan. We focus on the comparison and impact studies of FORMOSAT-3/ COSMIC GPS radio occultation (RO) and dropsonde data on regional weather prediction. The WRF model and its 3DVAR component, WRF-Var, are

used for the evaluation of the forecast of heavy rainfall events in Taiwan during an 11-day period from 5 to 15 June of the 2007 Mei-yu season.

2. Model designs

The WRF-ARW v2.2 model is used for model simulation. There are four experiments designed for this study. The control experiment (CON) uses the conventional (surface and sounding) observation data in the WRF-Var data assimilation. Three sensitivity

experiments are carried out. The GPS and DRP experiments use the data from FORMOSAT-3/COSMIC GPS RO and dropsonde observations, respectively, in the data assimilation. The ALL experiment ingests both of these two special data sets together. The GPS RO data include vertical profile of geopotential height, temperature, and moisture. The dropsonde data have one more field, which is wind. Table 1 shows the amount of available data during this 11-day period. The dropsonde data were mostly collected over the ocean near the southwest of Taiwan. Each experiment contains 22 runs of 72-h simulation. These runs were initialized twice daily from 0000 UTC 5 June 2007 to 1200 UTC 15 June 2007. The initial data of the first run at 0000 UTC 5 June 2007 were obtained from the NCEP GFS. The initial data of the other 21 runs were obtained from the 12-h update cycle of the previous WRF run. During the WRF-Var assimilation process, the available data shown in Table 1 were assimilated into the modeling system.

The domain settings include 2 domains with 45 and 15 km horizontal spacing and 31 levels in the vertical. The important physics processes of the WRF that were used in the study include the WRF Single-Moment 5-class microphysics scheme, the Kain-Fritsch cumulus parameterization scheme, and the YSU PBL scheme (Skamarock et al. 2005).

The verification was done by comparing the geopotential height (H), temperature (T), relative humidity (RH), and u- and v-wind components (U and V) with those of the best analyses from the NCEP initial fields plus

data assimilation of traditional observations. The correlation coefficient (CC), root-mean square error (RMSE), mean error (ME), and skill score (SS) are calculated for all the grid points in domain 2 and for all the 22 runs in the 11-day period. They are defined as follows,

$$CC = \frac{\frac{1}{N-1} \sum_{n=1}^N [(F_n - \bar{F})(O_n - \bar{O})]}{\left[\frac{1}{N-1} \sum_{n=1}^N (F_n - \bar{F})^2 \right]^{1/2} \left[\frac{1}{N-1} \sum_{n=1}^N (O_n - \bar{O})^2 \right]^{1/2}}$$

$$RMSE = \sqrt{\frac{\sum_{n=1}^N (F_n - O_n)^2}{N-1}},$$

$$ME = \frac{\sum_{n=1}^N (F_n - O_n)}{N}, \text{ and}$$

$$SS = -\frac{RMSE_{GPS} - RMSE_{CON}}{RMSE_{CON}} \times 100\%,$$

where F and O are the forecast and observation fields, respectively. N is the number of the sample size. Skill score is defined as the percentage improvement of a particular experiment (GPS or DRP) over the reference forecasts (CON). The results on three pressure levels (850, 500, and 300 hPa) are shown in this paper. In addition to these meteorological fields, we also perform verification of 12-h precipitation forecasts against the observation from the rain gauges in Taiwan. The ETS (equitable threat score) and bias are computed for verification. They are defined as follows,

$$ETS = \frac{H - R}{F + O - H - R},$$

$$Bias = \frac{F}{O},$$

where H is the number of hits, and F and O

are the numbers of samples in which the precipitation amounts are greater than the specified threshold in forecast and observation, respectively. The random forecast is $R = FO/N$, where N is the number of points being verified.

3. The results

Figure 2 shows correlation coefficient (CC) of the four experiments compared with the best analyses. For relative humidity (RH), the CCs of the GPS experiment are higher than those of the CON experiment at 850 hPa after longer integration, e.g., after 36 h. At 500 hPa, the GPS has higher CCs than the CON at all time. At 300 hPa, the GPS also has slightly higher CCs than the CON at most of the time. As for the DRP experiment, the CCs are not good at 850 hPa, but they are better than the CON at 500 and 300 hPa. With both the GPS RO and dropsonde data assimilated together, the ALL experiment has even higher CCs than the GPS and the DRP experiments for many time periods. The CCs are the highest at 500 hPa and the lowest at 300 hPa, and they decrease over time.

The CCs of geopotential height (H) show that the GPS experiment performs better than the CON at 850 hPa after 36 h. At higher levels (500 and 300 hPa), the similar trend is still observed. The CCs of the DRP at 850 hPa are higher than the CON at 12 and 24 h, but they become lower than the CON after 24 h. At 500 and 300 hPa, nearly all the CCs of the DRP are higher than the CON. Compared with those of the GPS, the CCs of the DRP tend to be higher at early time, but lower at later time. The ALL experiment has the

highest CCs, especially at longer integration time. These CCs are all quite high, especially at 300 hPa, for all experiments at earlier forecast time, and they decrease over time. The distribution of CCs of temperature (T) is very similar to that of the geopotential height. The CCs are also quite high, too.

The CCs of the u-component (U) at all levels show that the GPS experiment does not perform well at early time, but it becomes better after 24 h. The CCs of the DRP at low level (850 hPa) are mostly lower than those of the CON, but they are mostly higher at mid and high levels (500 and 300 hPa). At many time periods, they are even the best among these three experiments. The ALL experiment performs very well at many time periods. The CCs of the v-component (V) are quite similar to those of the u-component, except that they are slightly lower.

Figure 3 shows RMSE of the three experiments for all variables. It is clear that the relative performance of the experiments is quite similar to that shown in the CC distribution. The experiment which has higher CC possesses lower RMSE, and vice versa.

The MEs of the three experiments show (Fig. 4) that the model under-predicts moisture at 850 and 300 hPa. At 500 hPa, the MEs of RH are only slightly below zero. Compared with the large RMSEs from Fig. 3, these small MEs suggest that the forecasts of RH at 500 hPa are quite diverse. As for the relative performance of each experiment, the distribution is similar to that of RMSE.

The model also mostly under-predicts geopotential height (H). However, with the assimilation of the GPS data, the

under-estimate problem is reduced, especially at longer integration time. At early time, the GPS experiment slightly over-predicts the height. The MEs of temperature show a reverse pattern from the low to high levels. They are positive at 850 hPa, near zero at 500 hPa, and negative at 500 hPa. This suggests that the model has a warm bias at low level and a cold bias at high level.

The MEs of the u-component wind are mostly positive, but they are in general small. However, their RMSEs are not small, which means the distribution of the errors is diverse. Another interesting feature is the MEs exhibit a different pattern among the three experiments to the RMSEs. For example, the GPS experiment has the highest positive MEs, but its RMSEs are the lowest for most of the time periods. This suggests that the assimilation of the GPS data tends to increase the positive bias of the u-component, but it reduces the RMSEs. The v-component winds show a similar pattern with the u-component wind, but with the bias being negative.

Figure 5 shows skill score (SS) of the GPS experiment against the CON experiment. Basically, the SSs more clearly show the improvement or worsening of the particular experiment over the CON experiment. At 300 hPa, the GPS experiment shows positive SSs for geopotential height at all time periods, and the SS is the largest (~9%) at 24 h. The other variables do not have large improvement like geopotential height, but they still exhibit a trend of increasing SS at longer integration. At 72 h, the SSs are positive for all variables.

At 500 and 850 hPa, the GPS experiment still show, for almost all the variables, the

tendency of improving forecast skill at later forecast time. Geopotential height has consistently the largest SSs after 48 h of integration. Relative humidity has positive SSs at 500 hPa, but negative SSs at 850 hPa. It is thus clear that the GPS data can provide accurate information of pressure at all the three levels such that the simulation of geopotential height can be improved after longer integration. However, moisture provided by the GPS data is only good at high levels (e.g., 500 hPa). The low-level moisture which is important on precipitation formation is not good. It is also possible that the moisture analyses at 850 hPa are not good enough.

Compared with the GPS experiment (Fig. 5), the DRP experiment has lower SSs and it does not show the trend of improvement over time (Fig. 6), instead, the SSs are in general higher at early time and they decrease as integration time increasing. The assimilation of dropsonde data helps to improve the simulation for almost every variable at 300 and 500 hPa, but it does not improve the forecast at 850 hPa.

With both the GPS RO and the dropsonde data assimilated, the ALL experiment shows even higher SSs than both the GPS and the DRP experiments. The tendency of SS for each variable is very similar to that of the GPS experiment, except for small differences. This is because the dropsonde data are available only in 6 out of the 22 runs. Their impact is relatively small.

Figure 8 presents the ETS and bias of the rainfall forecast of the four experiments verified against the rain gauge observations in

Taiwan. At 12-24 h (B period), there is no improvement for the GPS and DRP experiments against the CON experiment. At 24-36 h (C period), both the GPS and DRP experiments predict better rainfall than the CON experiment at small thresholds (e.g., < 10 mm). The ALL experiment has even higher ETS than the other experiments. At higher thresholds, however, all the three experiments are worse than the CON. The results at 36-48 h and 48-60 h (D and E periods) show that the GPS experiment has the highest ETS at rainfall thresholds smaller than 15 mm. The DRP experiment is also better than the CON, but only at very small thresholds like 0.3 and 2.5 mm. At 60-72 h (F period), the DRP experiment appears to have the highest ETS and the GPS experiment has the lowest ETS at rainfall thresholds larger than 2.5 mm.

4. Conclusions

The WRF model and its WRF-Var system are used to examine the impact of the COSMIC GPS data and the dropsonde data on the forecast of a heavy rainfall period (11 days) in Taiwan during the 2007 Mei-yu season. The results show that the assimilation

of the GPS data can help to improve the simulation at the time periods of longer integration (e.g., > 36 h). The forecast of geopotential height, among other variables, has the largest impact from the GPS data. The improvement of assimilating the dropsonde data is in general positive at earlier forecast time and its impact decreases over time. However, this improvement only shows up at high levels like 300 and 500 hPa. At 850 hPa, the dropsonde does not help improve forecasts. With both the GPS RO and the dropsonde data assimilated, the ALL experiment shows even higher SSs than both the GPS and the DRP experiments. At 12-24 h, there is no improvement of rainfall forecasts for the GPS and DRP experiments against the CON experiment. However, when the integration time getting longer, the GPS and dropsonde data starts to help the rainfall simulation, especially for small rain thresholds. At 36-48 h and 48-60h, the GPS data significantly help to improve the rainfall prediction at rainfall thresholds smaller than 15 mm. The DRP and the ALL experiments are only slightly better than the control experiment.

Table 1: The amounts of data (SYNOP, SOUND, GPS, and dropsonde) used in the WRF-Var data assimilation for the 22 runs during the 11-day period.

| Init time (dd/hh) | 05/ 00 | 05/ 12 | 06/ 00 | 06/ 12 | 07/ 00 | 07/ 12 | 08/ 00 | 08/ 12 | 09/ 00 | 09/ 12 | 10/ 00 | 10/ 12 |
|----------------------|-----------|-----------|-----------|-----------|-----------|-----------|-----------|-----------|-----------|-----------|-----------|-----------|
| SYNOP | 914 | 964 | 877 | 882 | 898 | 973 | 902 | 902 | 917 | 915 | 916 | 959 |
| SOUND | 155 | 140 | 155 | 141 | 153 | 140 | 153 | 138 | 151 | 141 | 152 | 140 |
| GPS | 9 | 17 | 10 | 20 | 5 | 14 | 10 | 28 | 15 | 20 | 11 | 24 |
| Dropsonde | 13 | 0 | 13 | 0 | 8 | 0 | 8 | 0 | 13 | 0 | 7 | 0 |

| Init time (dd/hh) | 11/ 00 | 11/ 12 | 12/ 00 | 12/ 12 | 13/ 00 | 13/ 12 | 14/ 00 | 14/ 12 | 15/ 00 | 15/ 12 |
|----------------------|-----------|-----------|-----------|-----------|-----------|-----------|-----------|-----------|-----------|-----------|
| SYNOP | 904 | 908 | 899 | 914 | 898 | 900 | 891 | 900 | 892 | 927 |
| SOUND | 152 | 132 | 152 | 138 | 155 | 139 | 151 | 136 | 153 | 135 |
| GPS | 9 | 21 | 8 | 18 | 4 | 20 | 17 | 24 | 12 | 22 |
| Dropsonde | 0 | 0 | 0 | 0 | 0 | 0 | 0 | 0 | 0 | 0 |

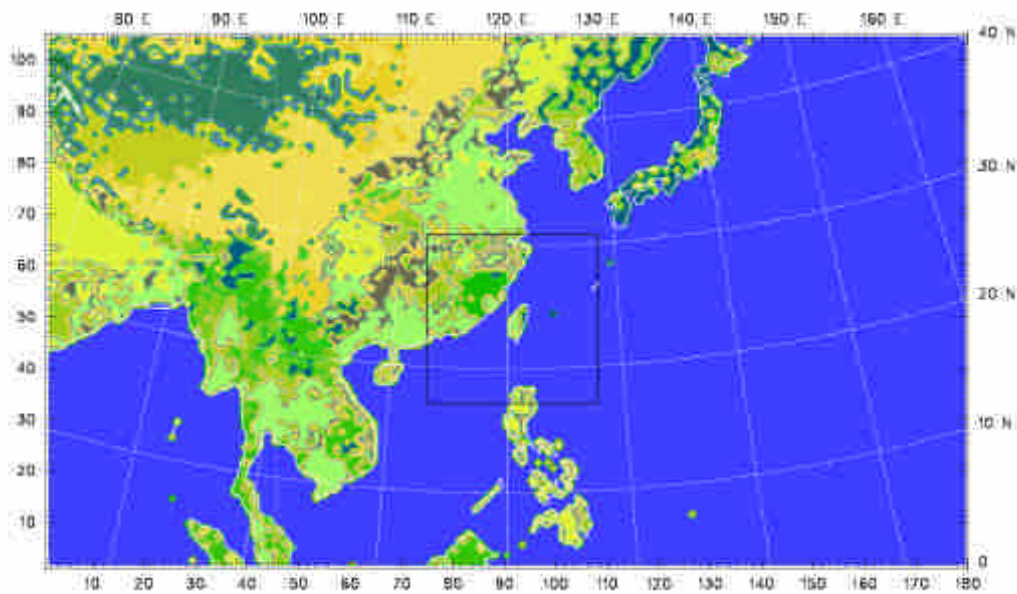


Fig. 1. The domain settings. Horizontal spacings for D1 and D2 are 45 and 15 km.

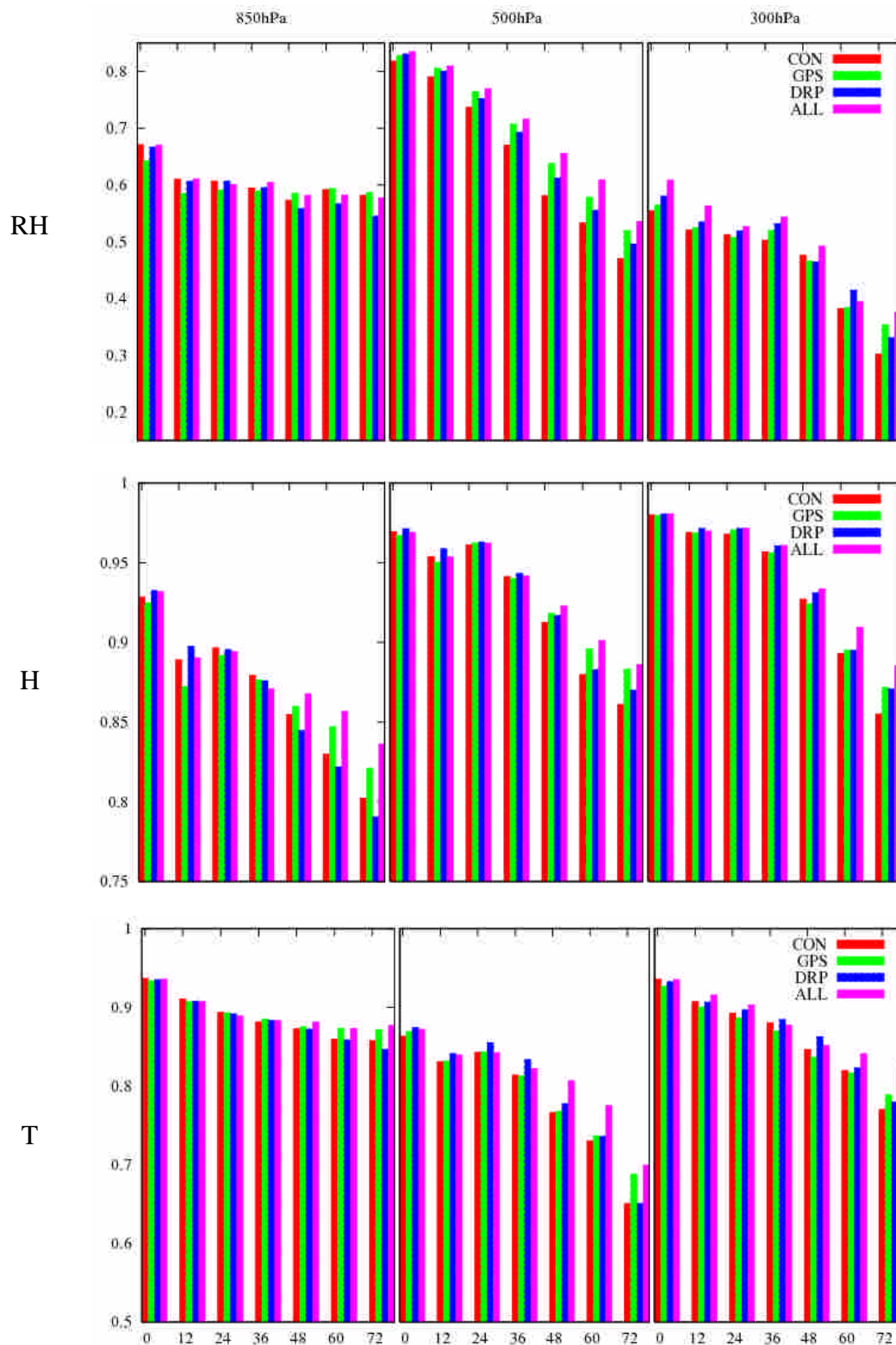


Fig. 2. Correlation coefficient (CC) of RH, H, T, U, and V for domain 2. Columns from left to right are results at 850, 500, and 300 hPa. The abscissa denotes time into the simulation (h). Color bars in red, green, blue, and magenta represent results for the CON, GPS, DRP, and ALL experiments.

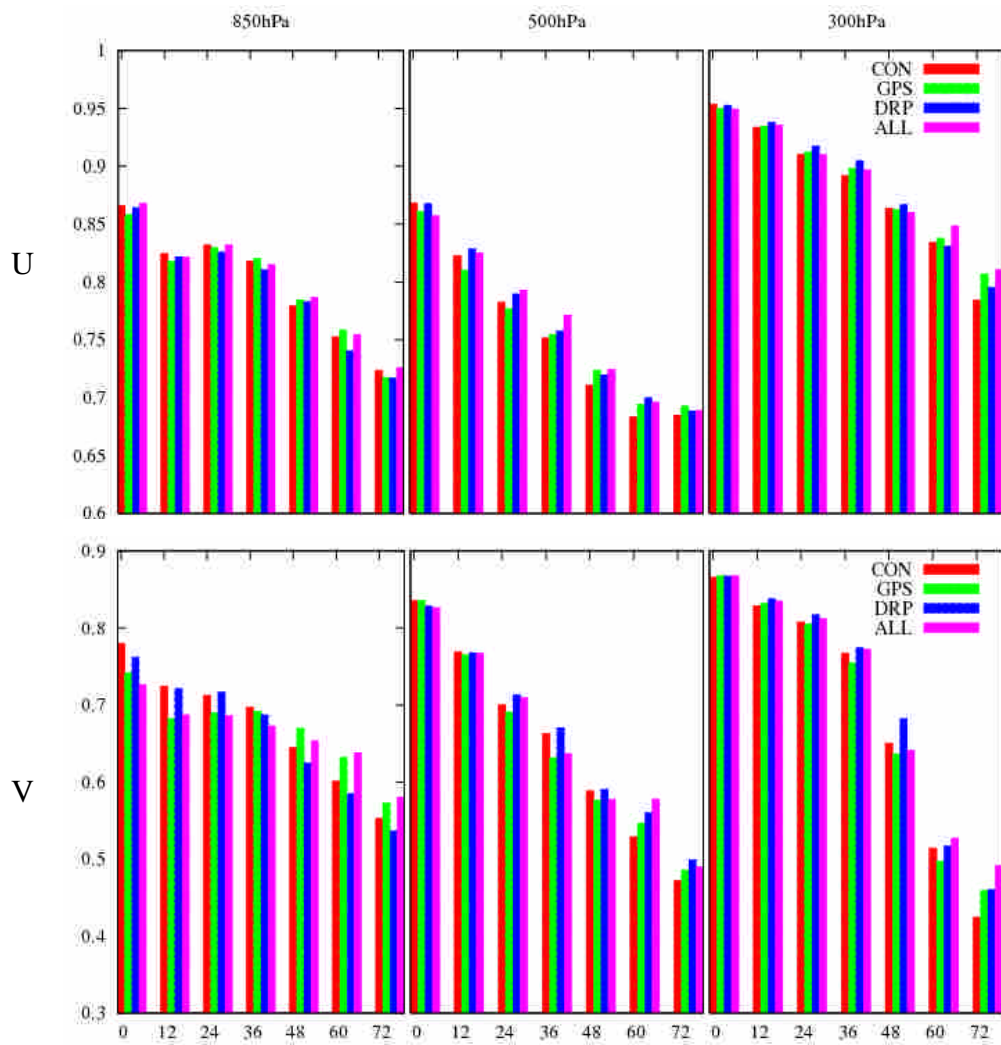


Fig. 2. (Continue).

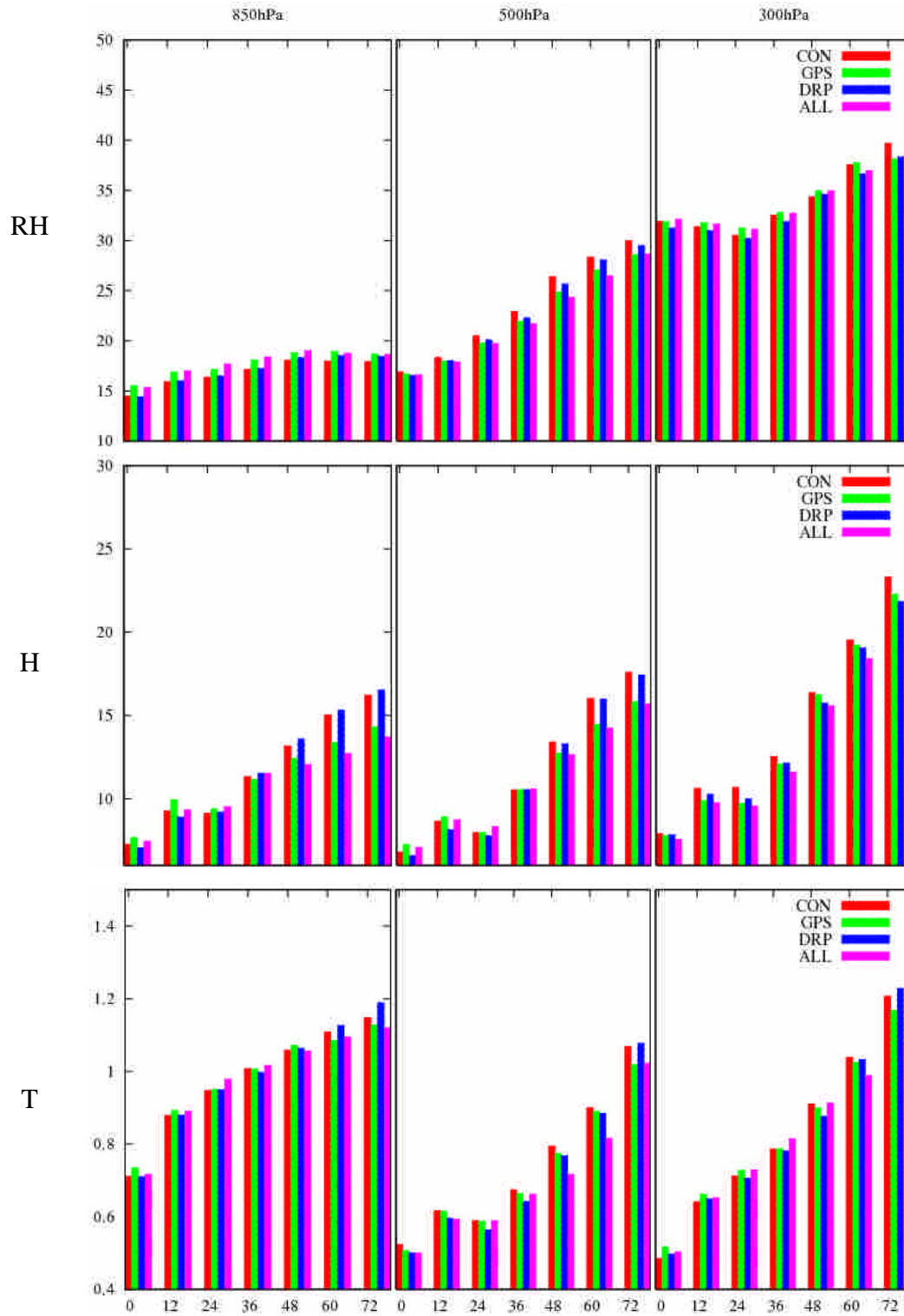


Fig. 3. Root-mean square error (RMSE) of RH (%), H (m), T ($^{\circ}$ C), U (m s^{-1}), and V (m s^{-1}) for domain 2. Columns from left to right are results at 850, 500, and 300 hPa. The abscissa denotes time into the simulation (h). Color bars in red, green, blue, and magenta represent results for the CON, GPS, DRP, and ALL experiments.

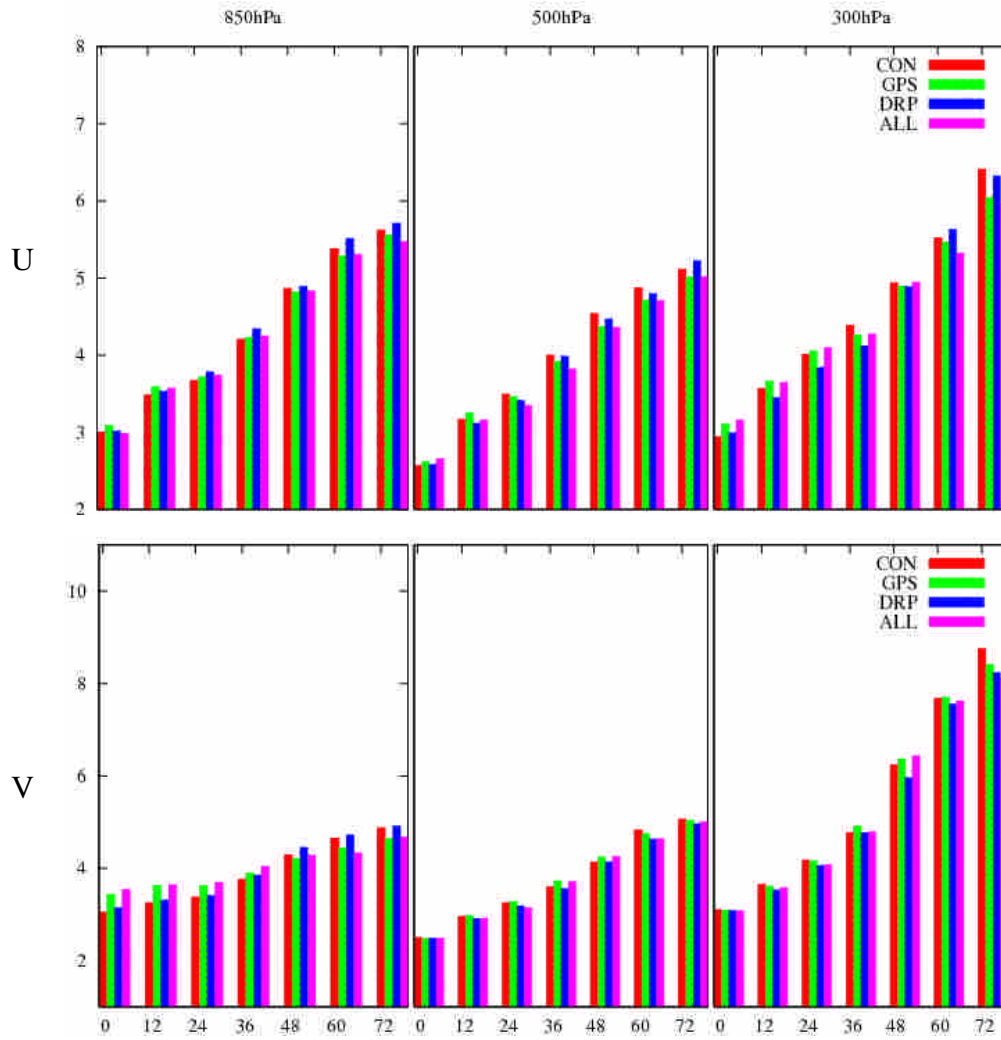


Fig. 3. (Continued).

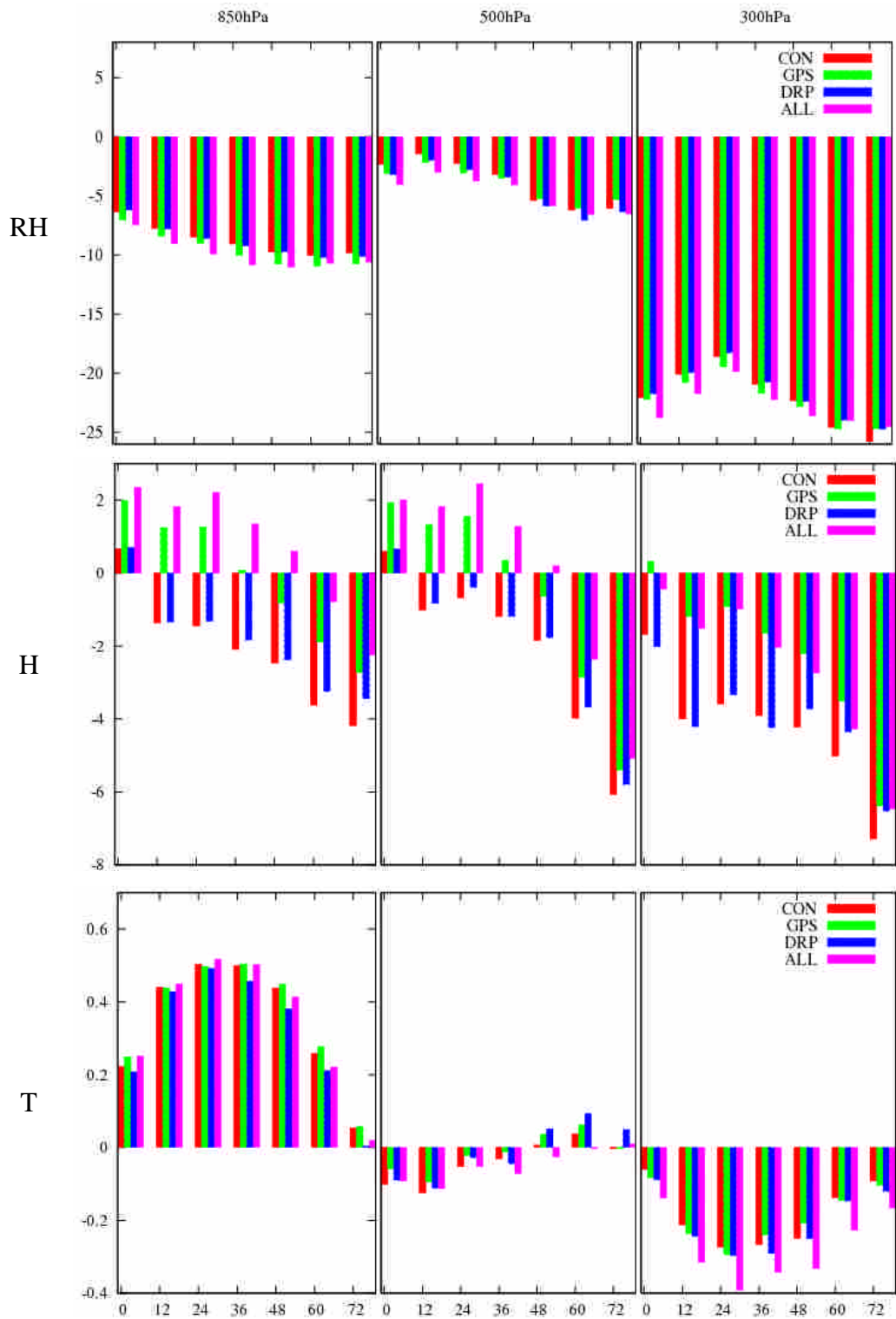


Fig. 4. Same as Fig. 3, but for mean error (ME).

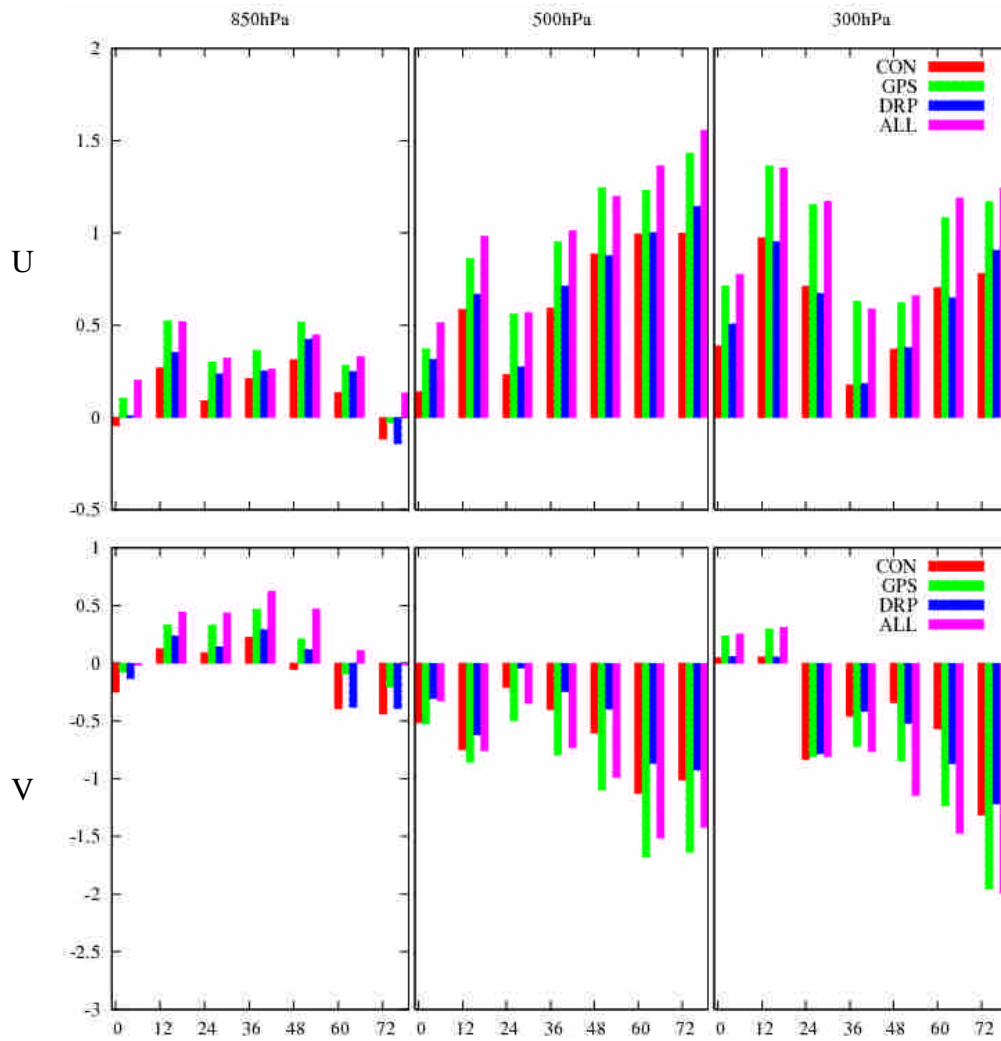


Fig. 4. (Continued).

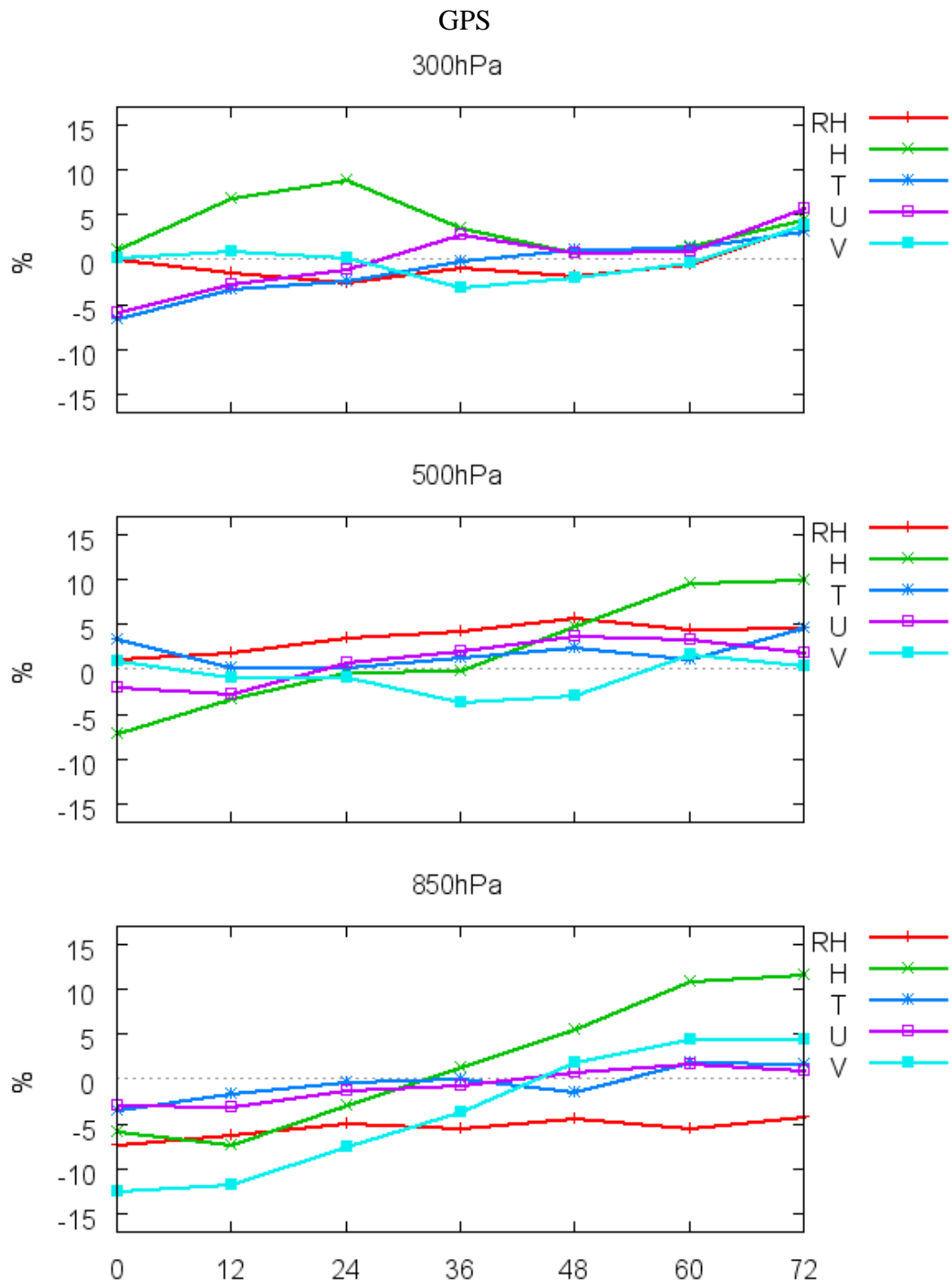


Fig. 5. Skill score for the GPS experiment against the CON experiment at 300, 500, and 850 hPa. The abscissa denotes time into the simulation (h). Color curves in red, green, blue, magenta, and cyan represent results for of RH, H, T, U, and V.

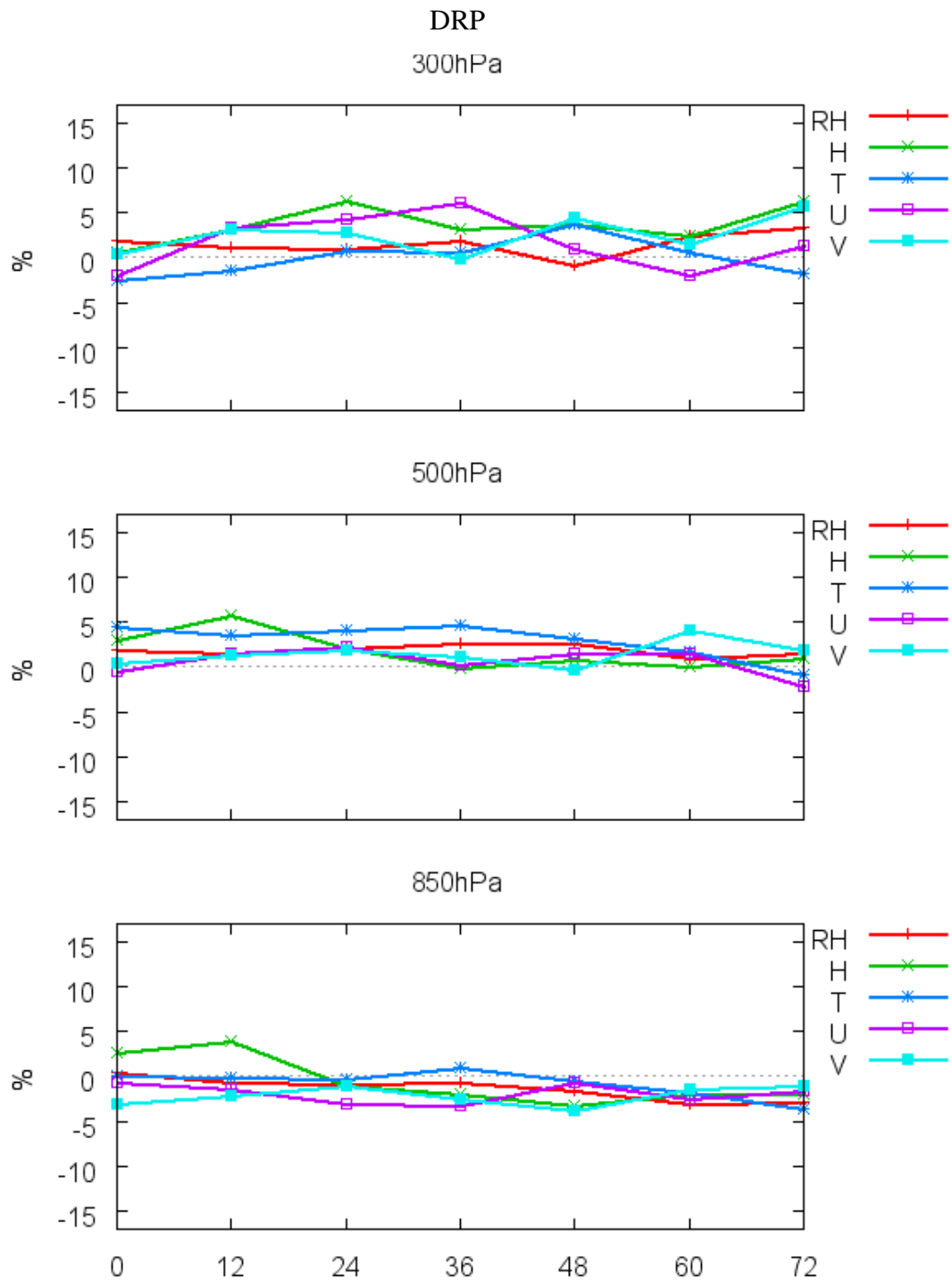


Fig. 6. Same as Fig. 5, but for the DRP experiment.

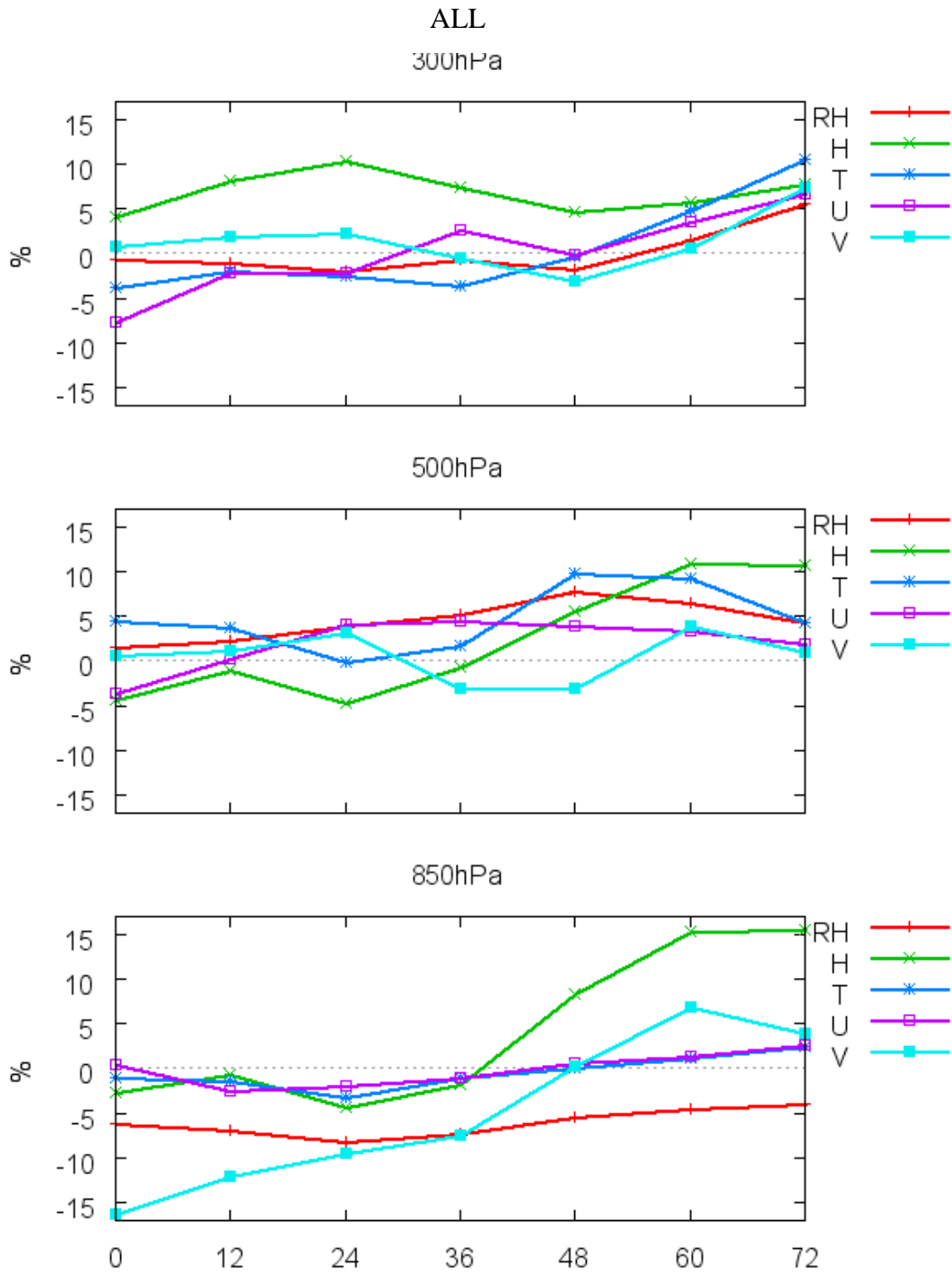


Fig. 7. Same as Fig. 5, but for the ALL experiment.

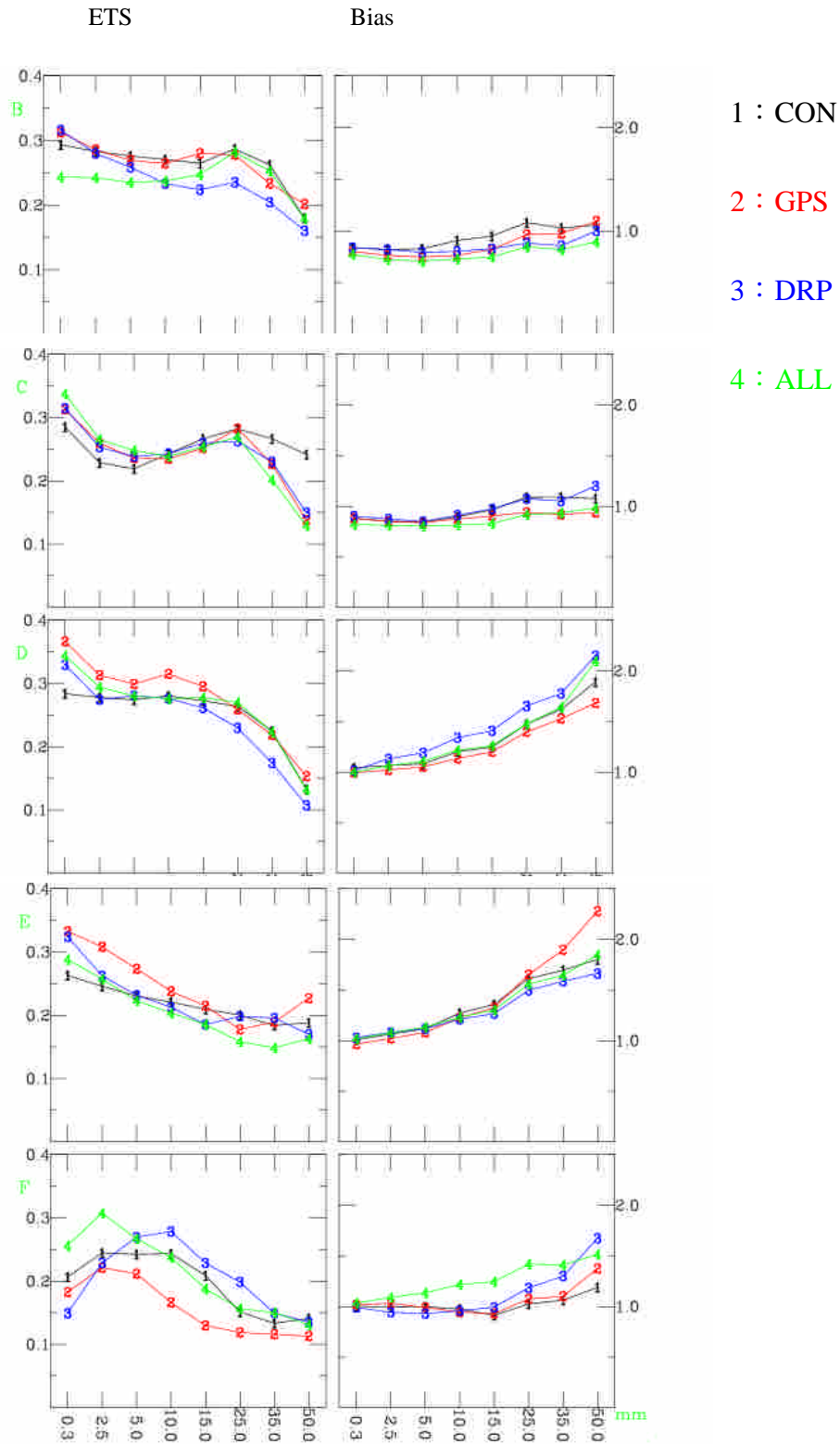


Fig. 8. The ETS (left) and bias (right) of 12-h precipitation forecasts from the CON (black, #1), GPS (red, #2), DRP(blue, #3), and ALL (green, #4) experiments. The abscissa is the rainfall thresholds (mm). Time periods B-F denote 12-h rainfall verification at 12-24 h, 24-36 h, 36-48 h, 48-60 h, 60-72 h, respectively.